

Metal-metal bonding in the KSbO_3 -type oxides $\text{La}_4\text{Ru}_6\text{O}_{19}$ and $\text{La}_3\text{Ru}_3\text{O}_{11}$: A mechanism for band gap formation in t_{2g} states

P. Khalifah and R. J. Cava

Department of Chemistry and Princeton Materials Institute, Princeton University, Princeton, New Jersey 08540

(Received 19 March 2001; published 7 August 2001)

The electronic structures of $\text{La}_3\text{Ru}_3\text{O}_{11}$ and $\text{La}_4\text{Ru}_6\text{O}_{19}$ were calculated using a LMTO-ASA-TB method. Although both compounds have similar conduction networks, $\text{La}_3\text{Ru}_3\text{O}_{11}$ was found to have a very normal band structure while $\text{La}_4\text{Ru}_6\text{O}_{19}$ showed many striking features. The t_{2g} band is split into three portions of clearly defined orbital origin. The two highest-energy portions are extremely narrow (~ 0.15 eV), and each have a capacity of only 1 electron per Ru atom. The highest portion of the t_{2g} band is separated from the remainder of the band by a gap of 0.5 eV. All these features occur in the absence of Jahn-Teller distortions. The origin of the gap is instead found to lie in metal-metal bonding due to the unusually short Ru-Ru distance in $\text{La}_4\text{Ru}_6\text{O}_{19}$ (2.5 Å vs 3.0 Å for $\text{La}_3\text{Ru}_3\text{O}_{11}$).

DOI: 10.1103/PhysRevB.64.085111

PACS number(s): 71.10.Hf, 71.20.-b

I. INTRODUCTION

Recent experimental results have shown that $\text{La}_4\text{Ru}_6\text{O}_{19}$ exhibits non-Fermi-liquid behavior while the structurally related compound $\text{La}_3\text{Ru}_3\text{O}_{11}$ does not.¹ An examination of the structures of these two compounds shows that a major difference between them is that $\text{La}_4\text{Ru}_6\text{O}_{19}$ has a short Ru-Ru distance of 2.5 Å indicative of metal-metal bonding,² while $\text{La}_3\text{Ru}_3\text{O}_{11}$ has a long Ru-Ru distance of 3.0 Å that precludes direct Ru-Ru interactions.^{3,4} Here we present electronic structure calculations on these two compounds. The differences we observe offer insights into the effects of metal-metal bonding on the previously measured physical properties.

The structures of $\text{La}_4\text{Ru}_6\text{O}_{19}$ and $\text{La}_3\text{Ru}_3\text{O}_{11}$ are presented in Fig. 1. $\text{La}_4\text{Ru}_6\text{O}_{19}$ has primitive cubic symmetry ($Pn\bar{3}$),² while $\text{La}_3\text{Ru}_3\text{O}_{11}$ has body-centered cubic symmetry ($I23$).^{3,4} Each unit cell contains the $M_{12}O_{36}$ cluster ($M = \text{Ru}$) common to the KSbO_3 structure type, which is the electronically active portion of the structure. The $M_{12}O_{36}$ clusters are virtually identical in $\text{La}_4\text{Ru}_6\text{O}_{19}$ and $\text{La}_3\text{Ru}_3\text{O}_{11}$ despite the different space groups and stoichiometries of these compounds. The twelve Ru atoms in each cluster are arranged into six dimers of edge-sharing RuO_6 octahedra. Dimers are a relatively rare structural motif in solid state compounds. Both compounds have the same formal charge of +4.33 per Ru.

In perovskites such as SrRuO_3 and CaRuO_3 , conduction electrons move through the Ru-O-Ru superexchange pathways between corner-sharing RuO_6 octahedra. When octahedra share edges, there is a possibility that the central metals will also interact via direct exchange pathways. Each edge-sharing dimer in $\text{La}_4\text{Ru}_6\text{O}_{19}$ and $\text{La}_3\text{Ru}_3\text{O}_{11}$ has four connections to other dimers through corner-shared oxygens, leading to a mix of Ru-Ru (J) and Ru-O-Ru (J') interactions, as shown in Fig. 1(c). Thus there is a strong possibility that competition between superexchange and direct exchange interactions will give rise to complex electronic and magnetic properties in these two compounds. We briefly note that the spin interactions in both of these compounds are analogous

to those in the spin gap compound $\text{SrCu}_2(\text{BO}_3)_2$,⁵ as these systems have one direct exchange interaction across the shared edge of a dimer and four superexchange interactions through corner-shared oxygens. The electronic structures of $\text{La}_4\text{Ru}_6\text{O}_{19}$ and $\text{La}_3\text{Ru}_3\text{O}_{11}$ were calculated in order to determine the extent and importance of direct exchange interactions in the presence and absence of Ru-Ru bonding.

II. EXPERIMENTAL

Band structure calculations were performed using the program LMTO47c developed by Andersen and co-workers.^{6,7} The program employs a LMTO-ASA (linear muffin-tin orbital, atomic sphere approximation) algorithm within the tight binding approximation. All relativistic effects except spin-orbit coupling were included in the calculations. Integrations over k space were performed using the tetrahedron method with a total of 45 ($\text{La}_3\text{Ru}_3\text{O}_{11}$) or 52 ($\text{La}_4\text{Ru}_6\text{O}_{19}$) irreducible k points from an 8 by 8 by 8 grid of reducible k points. Coordinates of the high symmetry points used for $\text{La}_3\text{Ru}_3\text{O}_{11}$ ($Pn\bar{3}$ symmetry) are Γ (000), M ($\frac{1}{2}\frac{1}{2}0$), X ($\frac{1}{2}00$), R ($\frac{1}{2}\frac{1}{2}\frac{1}{2}$), in units of $2\pi/a$. The high symmetry points for the $\text{La}_4\text{Ru}_6\text{O}_{19}$ ($I23$ symmetry) are Γ (000), N ($\frac{1}{2}\frac{1}{2}0$), P ($\frac{1}{2}\frac{1}{2}\frac{1}{2}$), H (010), in units of $2\pi/a$. Twice as many Ru atoms (12 vs 6) were present in the primitive cubic unit cell of $\text{La}_3\text{Ru}_3\text{O}_{11}$ as in the unit body-centered cubic unit cell of $\text{La}_4\text{Ru}_6\text{O}_{19}$. The orbital-weighted fatbands (discussed in more detail later) were obtained by averaging the results for three separate Ru atoms contained in dimers oriented with the Ru-Ru bond parallel to the x , y , and z axes. The atomic positions of $\text{La}_4\text{Ru}_6\text{O}_{19}$ (Ref. 2) and $\text{La}_3\text{Ru}_3\text{O}_{11}$ (Ref. 4) are given in Table I.

III. RESULTS AND DISCUSSION

The results of the electronic structure calculations for both compounds are presented in Figs. 2 and 3. The band structure of $\text{La}_3\text{Ru}_3\text{O}_{11}$ (Fig. 2) shows the presence of a broad manifold of states in a band which crosses E_F . These states are

TABLE I. Atomic positions of $\text{La}_4\text{Ru}_6\text{O}_{19}$ (Ref. 2) and $\text{La}_3\text{Ru}_3\text{O}_{11}$ (Ref. 4).

$\text{La}_3\text{Ru}_3\text{O}_{11}$ ($Pn\bar{3}$)					$\text{La}_4\text{Ru}_6\text{O}_{19}$ ($I23$)				
Atom	Wyck.	x	y	z	Atom	Wyck.	x	y	z
La1	4c	0.5	0.5	0.5	La	8c	0.16279	0.16279	0.16279
La2	8e	0.1129	0.1129	0.1129					
Ru	12g	0.09160	0.75	0.75	Ru	12e	0.36147	0.5	0
O1	12f	0.6203	0.25	0.25	O1	12d	0.33313	0	0
O2	24h	0.4169	0.7462	0.0397	O2	2a	0	0	0
O3	8e	0.3559	0.3559	0.3559	O3	24f	0.34044	0.28582	0.97122

made from highly hybridized mixtures of oxygen $2p$ orbitals and Ru t_{2g} orbitals, and their integrated density of states (DOS) shows that the manifold can hold a total of 6 electrons per Ru. As would be expected from simple electron counting, the t_{2g} manifold is partially filled to a level of 3.67 electrons per Ru. This is in accord with the experimentally observed metallic conductivity.¹ The total DOS (Fig. 3) shows no unusual features.

The electronic structure of $\text{La}_4\text{Ru}_6\text{O}_{19}$ has some significantly different features from that of $\text{La}_3\text{Ru}_3\text{O}_{11}$, suggesting that the metal-metal bonding may profoundly affect the properties of this compound. The band structure diagram (Fig. 2) shows that the $\text{La}_4\text{Ru}_6\text{O}_{19}$ t_{2g} manifold is split into three parts. The lowest portion is about 1 eV wide and has room for 4 electrons per Ru, as seen in the DOS plot (Fig. 3). The Fermi energy is found near the top of this broad band which is responsible for the metallic conductivity of $\text{La}_4\text{Ru}_6\text{O}_{19}$. The remaining two portions of the t_{2g} manifold occur as very narrow bands (0.15 eV in width) found 0.2 and 0.9 eV above E_F , and each portion has room for 1 electron per Ru atom. Remarkably, the DOS for the lower of these two narrow bands is almost as high as the DOS of the La $4f$ states (which are found 5 eV above E_F).

For $4d$ transition metals which are octahedrally coordinated by oxygen, the standard view of the electronic structure is that crystal field effects will split the five d bands into threefold degenerate t_{2g} orbitals and doubly degenerate e_g orbitals. For certain $3d$ transition metals, Jahn-Teller distortions can break the octahedral symmetry and further reduce

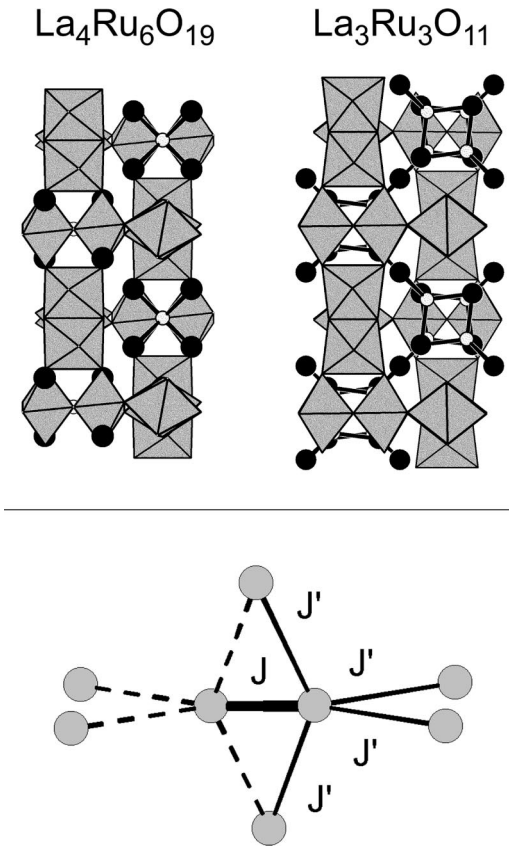


FIG. 1. Top: Structures of $\text{La}_4\text{Ru}_6\text{O}_{19}$ and $\text{La}_3\text{Ru}_3\text{O}_{11}$. RuO_6 octahedra are shown in gray. Large black circles are La atoms; small gray circles are O atoms. Bottom: Nearest neighbor spin interactions. J is the intradimer interaction and is expected to be strong for $\text{La}_4\text{Ru}_6\text{O}_{19}$ and weak for $\text{La}_3\text{Ru}_3\text{O}_{11}$. The interdimer interaction J' should be approximately the same for both compounds. Gray circles are Ru atoms. Thick line denotes direct exchange pathway across a Ru-Ru bond, while thin lines mark oxygen-mediated superexchange pathways.

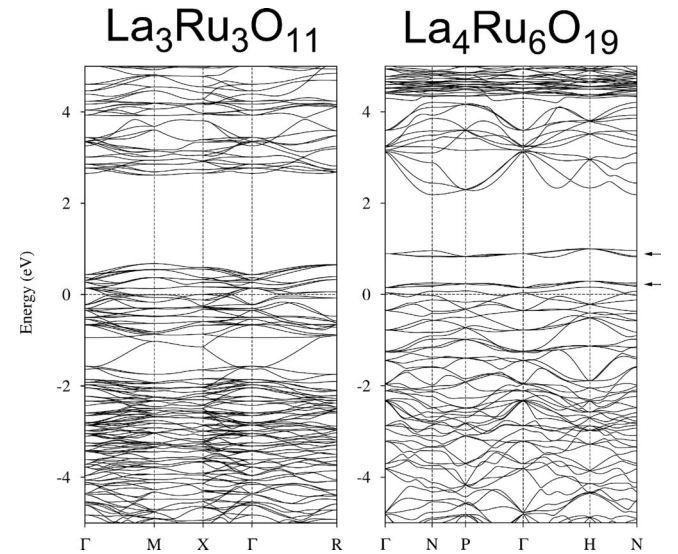


FIG. 2. Left: Band structure of $\text{La}_3\text{Ru}_3\text{O}_{11}$. Coordinates of high symmetry points are Γ (000), M ($\frac{1}{2}\frac{1}{2}0$), X ($\frac{1}{2}00$), R ($\frac{1}{2}\frac{1}{2}\frac{1}{2}$). Right: Band structure of $\text{La}_4\text{Ru}_6\text{O}_{19}$. Coordinates of high symmetry points are Γ (000), N ($\frac{1}{2}\frac{1}{2}0$), P ($\frac{1}{2}\frac{1}{2}\frac{1}{2}$), H (010). Arrows indicate one-electron bands. The Fermi energy is at 0 eV in both plots.

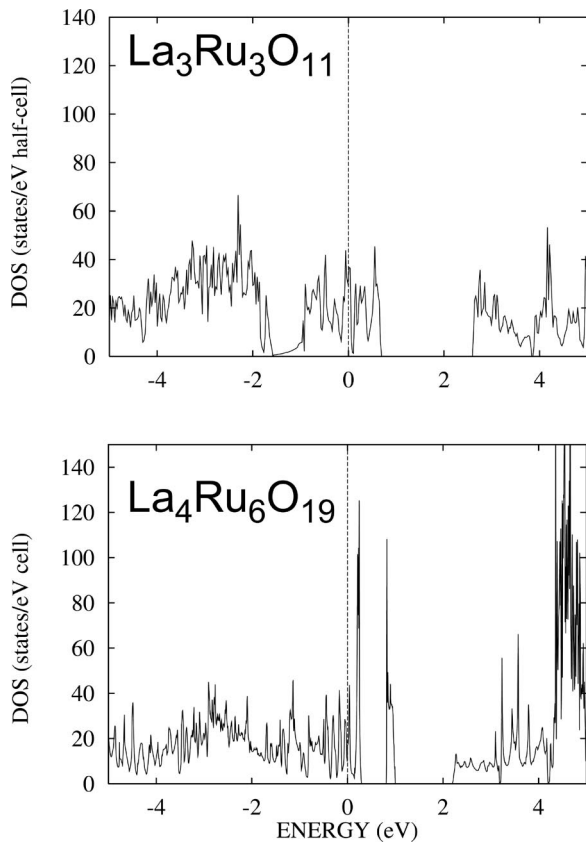


FIG. 3. Top: DOS plot for $\text{La}_3\text{Ru}_3\text{O}_{11}$. Bottom: DOS plot for $\text{La}_4\text{Ru}_6\text{O}_{19}$. The Fermi energy is at 0 eV in both plots.

the degeneracy of the d orbitals. However, Jahn-Teller distortions are energetically unfavorable for $4d$ transition metal oxides and the t_{2g}/e_g orbital model is almost universally followed. Furthermore, the RuO_6 octahedra were found to be undistorted in the original crystal structure determination of $\text{La}_4\text{Ru}_6\text{O}_{19}$ (Ref. 2) (solved by single crystal x-ray diffraction), as seen in the exceptionally narrow range of Ru-O bond distances (1.948 to 1.967 Å). A recent redetermination of the $\text{La}_4\text{Ru}_6\text{O}_{19}$ structure by powder neutron diffraction confirms the uniformity of the Ru-O distances to better than 0.01 Å.⁸ Thus the splitting of the Ru t_{2g} band seen in the band structure of $\text{La}_4\text{Ru}_6\text{O}_{19}$ is completely unexpected. Another very unusual feature is the low capacity (1 electron per Ru atom) of the two topmost t_{2g} subbands, which are at first glance incompatible with Fermi statistics, which dictate that two electrons may occupy any given orbital. This indicates that hybridization between the d orbitals of the two Ru atoms in each dimer has occurred. Thus the bands with a capacity of 1 electron per Ru are better thought of as molecular orbital-derived bands with a capacity of two electrons per dimer.

Previous electronic structure calculations on metal-metal bonding within the framework of organometallic molecules with similar geometries^{9–11} provide a convenient starting point for understanding the effects of metal-metal bonding in the periodic lattice of $\text{La}_4\text{Ru}_6\text{O}_{19}$. Within the edge-sharing dimers of octahedra, three types of orbital hybridization are possible, allowing bonds of up to order 3. The three t_{2g} or-

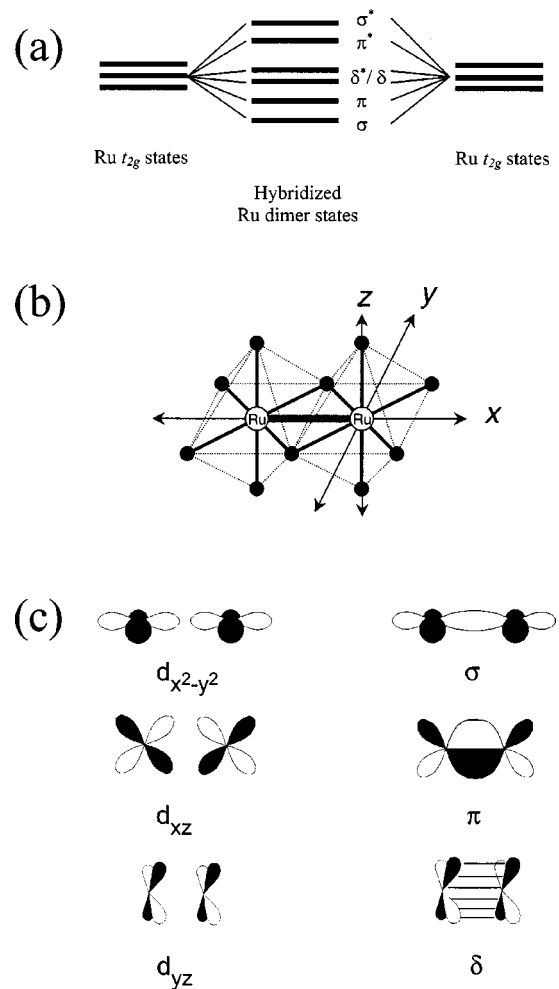


FIG. 4. (a) Molecular orbital ordering scheme for typical compounds with edge-sharing octahedra. (b) Nonstandard axis choice used for defining the Ru d -orbital directions. (c) Depiction of the d -orbital hybridization which gives rise to σ , π , and δ -type bonding interactions.

bitals from each metal atom hybridize to form six hybrid states of $\sigma, \pi, \delta, \delta^*, \pi^*$, and σ^* character, listed in approximate order of increasing energy. This molecular bonding scheme is drawn in Fig. 4(a).

It is worth noting that even within a periodic lattice, if the separation of molecular orbitals remains large relative to the bandwidths then the d orbital degeneracy can be completely lifted. This leads to a sharp reduction of the maximum magnetic moment from the t_{2g} derived states to a mere $S=1/2$ per dimer of metal atoms, regardless of the filling level. This is much less than the upper limit of $S=3/2$ per atom for low-spin transition metals or $S=5/2$ per atom for high-spin transition metals. In the specific case of $\text{La}_4\text{Ru}_6\text{O}_{19}$, metal-metal bonding should reduce the number of unpaired electrons to two electrons, each with $S=1/2$, for every three ruthenium dimers. This reduction in moment would be consistent with experimental measurements of the susceptibility of $\text{La}_4\text{Ru}_6\text{O}_{19}$, which has a maximum susceptibility of only $\sim 1 \times 10^{-3}$ emu/mol Ru, and whose susceptibility at all temperatures is much lower than would be expected for

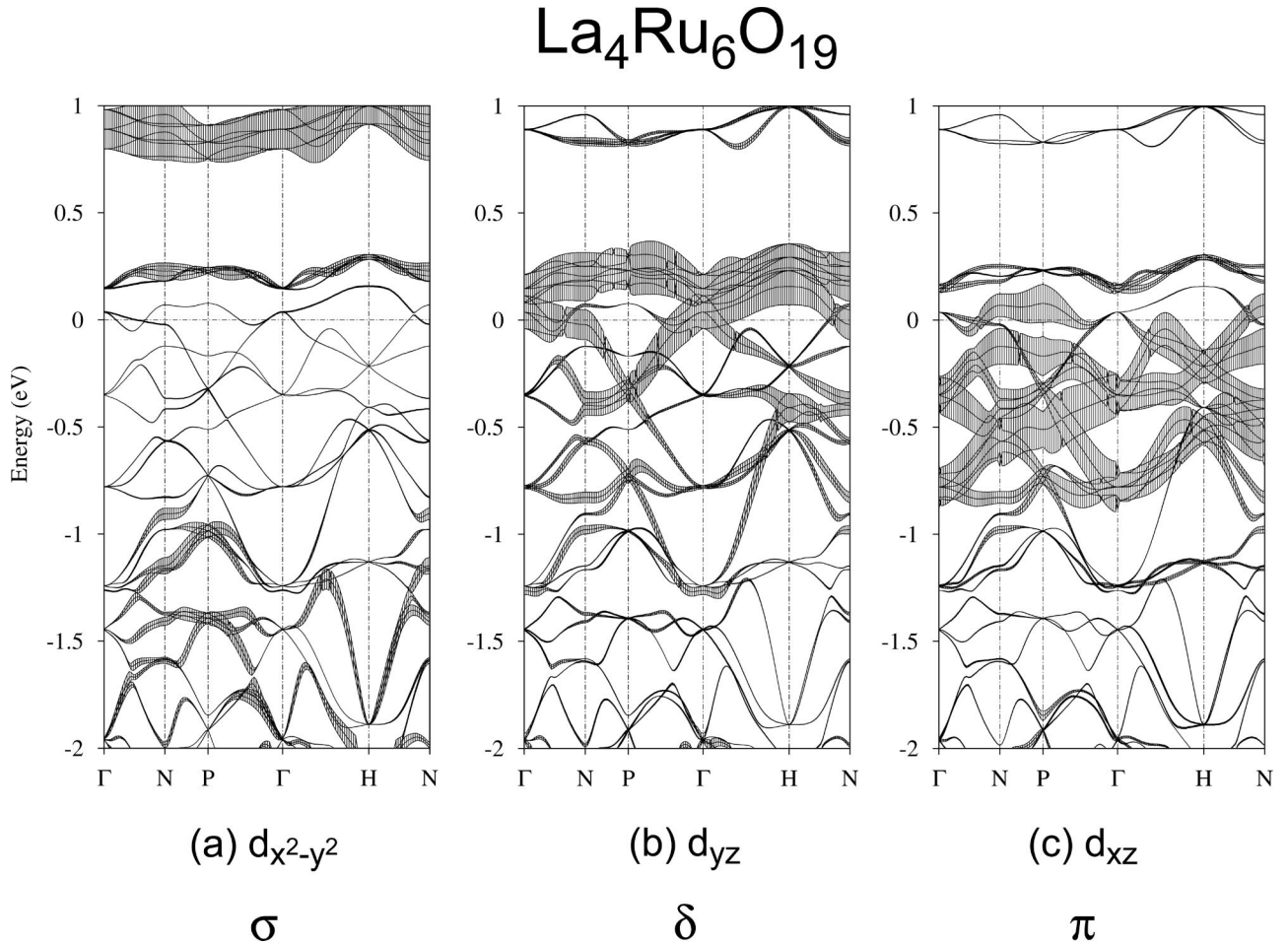


FIG. 5. Orbital-weighted bands (fat bands) for $\text{La}_4\text{Ru}_6\text{O}_{19}$. Lower label indicates the symmetry of the hybridized orbitals. Labels of high symmetry points are the same as in Fig. 2. The Fermi energy is at 0 eV in all plots.

$\text{Ru}^{4.33}$ in a typical octahedral environment.

Furthermore, in this degeneracy-lifted situation, any integer oxidation state of the transition metal will give an even number of electrons in the dimer's molecular orbitals, resulting in completely filled bands. Such compounds would be expected to have no paramagnetic moment, and perhaps even semiconducting behavior. The net effect of this situation would therefore be analogous to a Mott-Hubbard gap, although orbital hybridization resulting from metal-metal bonding rather than electron correlations would drive the opening of the gap.

The d orbitals involved in metal-metal bonding in $\text{La}_4\text{Ru}_6\text{O}_{19}$ are best described using a nonstandard coordinate axis choice, as depicted in Fig. 4(b). The x -axis is taken to lie along the metal-metal bond while the z -axis points toward the apical ligands, which corresponds to a rotation of 45° about the z -axis from the standard octahedral choice of axes. In terms of the crystal field splitting, t_{2g} states now have their origin in the $d_{x^2-y^2}$, d_{xz} , and d_{yz} orbitals, while the e_g states (which point toward oxygen atoms) arise from the d_{xy} and d_{z^2} orbitals.

Within each dimer, hybridization of two Ru $d_{x^2-y^2}$ orbitals gives rise to a σ and σ^* molecular orbitals (MO's). Similarly, d_{xz} Ru orbitals are involved in π -type MO's and d_{yz}

orbitals in δ -type MO's, as seen in Fig. 4(c). Although these MO's will be broadened into bands in $\text{La}_4\text{Ru}_6\text{O}_{19}$, the concept of metal-metal bonding remains. Bond formation results in certain two-metal hybrid states being lowered in energy at the expense of others being raised. In the specific case of $\text{La}_4\text{Ru}_6\text{O}_{19}$, the uppermost unoccupied states in the t_{2g} manifold have been pushed 1 eV above E_F , 0.5 eV higher in energy than they are found in $\text{La}_3\text{Ru}_3\text{O}_{11}$. For partial fillings of the t_{2g} manifold, there will be an energetic advantage to this hybridization-induced rearrangement of energy levels.

The most convincing evidence that these two-metal hybrid orbitals (i.e., metal-metal bonds) are vigorously affecting the electronic structure of $\text{La}_4\text{Ru}_6\text{O}_{19}$ comes from the analysis of the individual orbital contributions to the various bands of interest (Fig. 5). In each of these "fatband" plots, the thickness of the band at each point in k space is proportional to the contribution of the orbital of interest ($d_{x^2-y^2}$, d_{xz} , or d_{yz}). The thickest bands in the fatband plots are due solely to the featured orbital, while the bands that are merely lines have no contribution from the featured orbital. The e_g -derived d orbitals make no contribution to the bands in the energy range shown, and are therefore not shown.

The highest energy t_{2g} -derived narrow bands (0.9 eV above E_F) originate from $d_{x^2-y^2}$ orbitals in the dimer. The

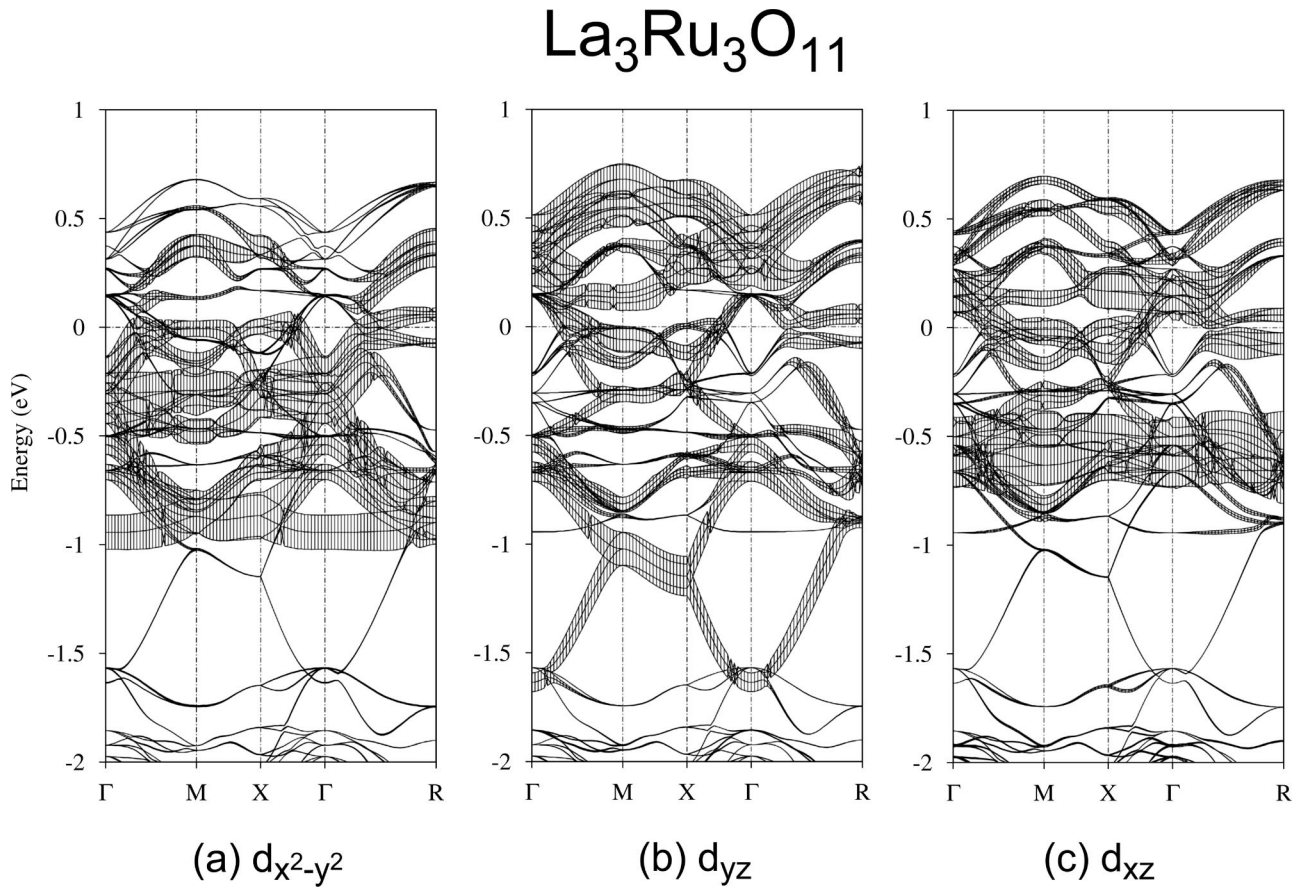


FIG. 6. Orbital-weighted bands (fatbands) for $\text{La}_3\text{Ru}_3\text{O}_{11}$. Labels of high symmetry points are the same as in Fig. 2. The Fermi energy is at 0 eV in all plots.

other set of narrow bands (0.2 eV above E_F) are of d_{yz} character, while the next lower set of states have d_{xz} character. The clear hierarchy of orbital energies seen in the figures is quite remarkable, and in the clear absence of Jahn-Teller distortions points to the importance of orbital hybridization. The energies of the molecular orbitals therefore follow the sequence $\sigma^* > \delta^* > \pi^*$ in the top half of the t_{2g} derived states in $\text{La}_4\text{Ru}_6\text{O}_{19}$. The remainder of the hybrid t_{2g} states (σ , π , δ) are not segregated and are well interspersed throughout the region below -1 eV, reflecting the Ru-O hybridization and demonstrating that these lower energy states are more typical of an extended solid than a molecular compound.

The orbital analysis of $\text{La}_3\text{Ru}_3\text{O}_{11}$ (Fig. 6) shows that the three t_{2g} orbitals ($d_{x^2-y^2}, d_{xz}, d_{yz}$) are well dispersed; each orbital is about 1 eV wide. Furthermore, the orbitals are not segregated and cross each other freely. This behavior is typical to conducting transition metal oxides. Thus the anomalous behavior of $\text{La}_4\text{Ru}_6\text{O}_{19}$ is due the orbital hybridization resulting from metal-metal bonding rather than simply being a peculiarity of the geometry of the KSbO_3 -type $\text{Ru}_{12}\text{O}_{36}$ conduction network.

It has been proposed that the magnetic behavior of $\text{La}_4\text{Ru}_6\text{O}_{19}$ may be indicative of a spin gap.¹ If the model of nondegenerate molecular orbitals is correct, then it is possible to envision a means for a spin gap to occur. The primitive cell of $\text{La}_4\text{Ru}_6\text{O}_{19}$ contains three Ru_2O_{10} dimers. Based on the electronic structure calculations described above, the

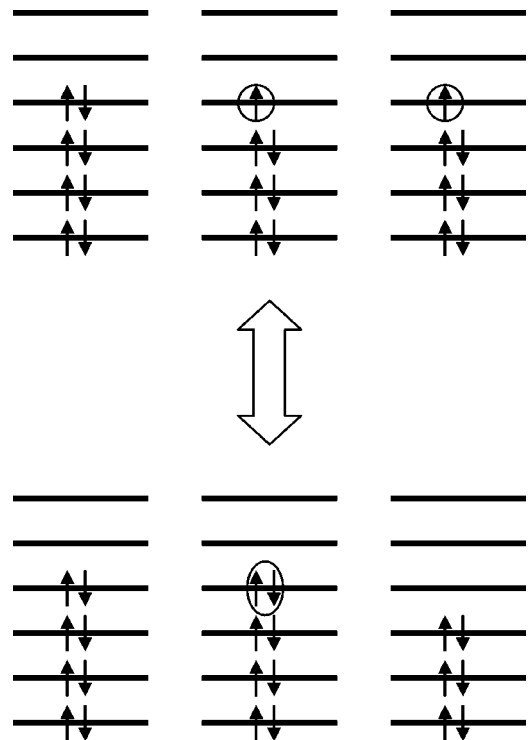


FIG. 7. Possible pathway for spin pairing in $\text{La}_4\text{Ru}_6\text{O}_{19}$. Top: Expected room-temperature electronic configuration of $\text{La}_4\text{Ru}_6\text{O}_{19}$. Bottom: Possible low-temperature ground state configuration with singlet spins.

expected electronic configuration within a single cell (Fig. 7, top) is $\sigma^2 \pi^2 \delta^2 \pi^{*1}$ for two of the dimers and $\sigma^2 \pi^2 \delta^2 \pi^{*2}$ for one of the dimers in each unit cell, giving $\text{La}_4\text{Ru}_6\text{O}_{19}$ a total of two unpaired spins per cell. If it is energetically favorable for the two spins to reside on the same dimer instead of on separate dimers, then $\text{La}_4\text{Ru}_6\text{O}_{19}$ will have a singlet ground state with two of the dimers with the $\sigma^2 \pi^2 \delta^2$ configuration and one with the $\sigma^2 \pi^2 \delta^2 \delta^{*2}$ configuration (Fig. 7, bottom). Chemically speaking, this pairing will occur if one Ru-Ru double bond and one Ru-Ru triple bond are more stable than two Ru-Ru bonds of order 2.5. An alternate perspective is that the energy gain for a dimer to have an empty π^* orbital exceeds the pairing energy for two π^* electrons to sit on the same dimer.

IV. CONCLUSIONS

In the absence of Jahn-Teller distortions, it is rare to find a large splitting of the energies of the t_{2g} orbitals in transition

metal oxides. However, our calculations show that metal-metal bonding provides a new mechanism for gap formation within the t_{2g} manifold, as hybridization of two sets of Ru d orbitals in $\text{La}_4\text{Ru}_6\text{O}_{19}$ leads to a lifting of degeneracy of the highest energy t_{2g} -derived states. As this hybridization is not found in the structurally related compound which lacks Ru-Ru bonding ($\text{La}_3\text{Ru}_3\text{O}_{11}$), metal-metal bonding is demonstrated to be a key feature responsible for the unique physical properties of $\text{La}_4\text{Ru}_6\text{O}_{19}$, much as Mott-Hubbard splitting inspires some of the anomalous features of layered cuprates.

ACKNOWLEDGMENTS

This work was supported by the National Science Foundation Grant No. DMR-9725979. P. K. gratefully acknowledges support from the National Science Foundation.

-
- ¹P. Khalifah, K.D. Nelson, R. Jin, Z.Q. Mao, Y. Liu, Q. Huang, X.P.A. Gao, A.P. Ramirez, and R.J. Cava *Nature (London)* **411**, 669 (2001).
²F. Abraham, J. Trehoux, and D. Thomas, *Mater. Res. Bull.* **12**, 43 (1977).
³F. Abraham, D. Thomas, and G. Nowogrocki, *Bull. Soc. Fr. Mineral. Cristallogr.* **98**, 25 (1975).
⁴F.A. Cotton and C.E. Rice, *J. Solid State Chem.* **25**, 137 (1978).
⁵H. Kageyama, K. Yoshimura, R. Stern, N.V. Mushnikov, K. Onizuka, M. Kato, K. Kosuge, C.P. Slichter, T. Goto, and Y. Ueda, *Phys. Rev. Lett.* **82**, 3168 (1999).

- ⁶O.K. Andersen and O. Jepsen, *Phys. Rev. Lett.* **53**, 2571 (1984).
⁷O.K. Andersen, Z. Pawłowska, and O. Jepsen, *Phys. Rev. B* **34**, 5253 (1986).
⁸P. Khalifah, Q. Huang, and R.J. Cava (unpublished).
⁹F.A. Cotton, M.P. Diebold, C.J. O'Connor, and G.L. Powell, *J. Am. Chem. Soc.* **107**, 7438 (1985).
¹⁰S. Shaik, R. Hoffmann, C.R. Fisel, and R.H. Summerville, *J. Am. Chem. Soc.* **102p**, 4555 (1980).
¹¹F.A. Cotton and R.A. Walton, *Multiple Bonds between Metal Atoms*, 2nd ed. (Clarendon Press, Oxford, 1993).